Electrocatalytic oxygen evolution by synergistically coupling layered double hydroxide Ni-based with MXene

Nurul Atiqah Izzati Md Ishak[1*], Saidur Rahman[2, 3], Norulsamani Abdullah[2], Azran Mohd Zainoodin[4], Adarsh Kumar Pandey[2, 3], Kim Han Tan[2] and Md Abu Zaed[2]

[1]Research Centre for Carbon Dioxide Capture and Utilisation (CCDCU), Faculty of Engineering and Technology, Sunway University, No. 5, Jalan Universiti, Bandar Sunway, Petaling Jaya, 47500, Selangor Darul Ehsan, Malaysia
[2]Research Centre for Nano-Materials and Energy Technology (RCNMET), School of Engineering and Technology, Sunway University, Bandar Sunway, Petaling Jaya, 47500, Selangor Darul Ehsan, Malaysia
[3]School of Engineering, Lancaster University, Lancaster, LA1 4YW, UK
[4]Fuel Cell Institute, Universiti Kebangsaan Malaysia, 43600 UKM Bangi, Selangor, Malaysia

[*]E-mail: atiqahmi@sunway.edu.my

Abstract. Electrolysis presents a cost-effective and environmentally friendly approach for producing carbon-neutral hydrogen, addressing global environmental challenges. However, the slow kinetics of the oxygen evolution reaction (OER) pose a significant obstacle in many sustainable energy conversion processes. In this study, a novel two-dimensional (2D) $Ti_3C_2T_x$ MXene substrate was used to hybridize with Mo-doped NiCo phosphate nanostructures through a two-step hydrothermal process followed by phosphating calcination, resulting in a low-cost and efficient electrocatalyst. The porous, defect-rich $Ti_3C_2T_x$ flakes provide metal-like electrical conductivity and a large surface area, supporting the direct growth of active species and improving their catalytic performance for the OER. The synthesized $Ni_1Co_1Mo_{0.125}Px$/MXene exhibited an overpotential of 314.6 mV at 10 mA cm^{-2} and a Tafel slope of 77 mV dec^{-1}, with an electrochemical double-layer capacitance (Cdl) of 7.1 μF cm^{-2} corresponding to a large electrochemically active surface area (ECSA). Electrochemical impedance spectroscopy (EIS) confirmed a low charge-transfer resistance, while chronoamperometry (CA) stability tests demonstrated robust long-term durability under continuous operation. This unique nanostructure enhances electrocatalytic activity due to the synergistic effects between the metal components, offering improved performance for the oxygen evolution reaction.

Keywords: Oxygen evolution reaction, Water electrolysis, Hydrogen energy, MXene composites, Transition metal phosphides

1. Introduction

The heavy reliance on fossil fuels has led to significant environmental issues, underscoring the need for net-zero emissions via renewable energy and sustainable practices. Hydrogen, particularly through alkaline electrolysis, is a promising alternative, with the oxygen evolution reaction (OER) being a crucial yet slow step, requiring noble metal oxides like IrO_2 and RuO_2 [1], [2]. However, these materials are expensive and scarce, hindering commercialization. To address this, researchers are developing cost-effective, efficient OER catalysts using earth-abundant elements such as the transition metal phosphides (TMPs) group of Ni and Co phosphides [3]. TMPs are particularly promising due to their abundance, high activity, stability, and low cost [4], [5].

Recently, researchers have looked into two-dimensional (2D) nanomaterials, like MXene ($Ti_3C_2T_x$), which has shown potential in enhancing OER activity due to its high electrical conductivity, large surface area, and excellent stability [6], [7]. Combining MXene with metal nanoparticles like TMPs can also serve as excellent supports for stabilizing catalysts, which in turn increases the OER by improving the charge transference, electrolyte accessibility, and electrochemical active surface area (ECSA). Implementing MXene with TMPs catalysts appears to have received little attention, especially in the electrocatalytic activity of OER for alkaline water electrolysis [3], [4], [5], [8].

To enhance the electrocatalytic activities, incorporating Mo into NiCo-based catalysts on MXene substrates also offers several advantages. Mo doping can modulate the electronic structure by shifting the d-band center, thereby optimizing the adsorption energies of oxygenated intermediates during OER [9]. Furthermore, Mo enhances structural stability by preventing Ni/Co leaching under alkaline conditions [10]. When coupled with highly conductive MXenes, the synergistic effect of Ni, Co, Mo, and P provides a favorable environment for rapid charge transfer and the generation of abundant active sites [11]. This combination is expected to significantly boost OER performance.

In this work, hierarchical molybdenum-doped-NiCo phosphatized on $Ti_3C_2T_x$ MXene composite is developed by adjusting the ratio of Co and Mo precursor to the Ni precursor using a simple hydrothermal and phosphating route as depicted in Fig. 1. The OER activity was stimulated by the modulation of Mo doped with the molar ratio $NiCoP_x$ electron structure through the interfacial interaction with MXene. The creation of effective and stable multicomponent catalysts can be guided by adjusting the interface interaction between the substrate and active components. The resulting $NiCoMoP_x$/MXene was characterized for its physicochemical and electrochemical properties, highlighting its promising potential as an efficient electrocatalyst for sustainable energy applications, particularly in water electrolysis, hydrogen production, and other renewable energy conversion systems.

2. Experimental

2.1 Synthesis of $Ti_3C_2T_x$ MXene

The Ti_3AlC_2 MAX phase (purity >98%, particle size <40 μm) was purchased from Carbon-Ukraine. The 1 g of MAX phase (Ti_3AlC_2) was mixed with 9 M HCl and 1.62 g of LiF to selectively etch the Al layers and stirred at 35 °C for 24 hours, then washed, centrifuged, and dried overnight in a vacuum oven at 60 °C to obtain the MXene, $Ti_3C_2T_x$.

2.2 Synthesis of layered double hydroxide Ni-based with MXene

10 mg of synthesized $Ti_3C_2T_x$ MXene were mixed with an aqueous solution containing 50 mL of $Ni(NO_3)_2{\cdot}6H_2O$, $Co(NO_3)_2{\cdot}6H_2O$, $Na_2MoO_4{\cdot}2H_2O$, with a series of regulating molar ratios of Co and Mo precursor with the addition of 100 mM ascorbic acid, 100 mM urea, and 80 mM ammonium fluoride. The mixture was stirred for 2 h, then transferred to a Teflon-lined stainless-steel autoclave and heated at 140 °C for 12 h. After cooling, the product was rinsed with deionized water and dried overnight at 60 °C. The resulting $NiCo_2O_4MoO_4$/MXene was placed in an alumina boat along with another boat containing 500 mg NaH_2PO_2. Both boats were calcined at 300 °C for 1 h under Ar flow, yielding hierarchical NiCoMoP/MXene. The electrocatalysts designated as $Ni_1Co_1Mo_{0.125}P$/MXene, $Ni_1Co_{0.75}Mo_{0.1}P$/MXene, $Ni_1Co_{0.5}Mo_{0.1}P$/MXene, and $Ni_1Co_{0.4}Mo0_{.1}P$/MXene, with a schematic diagram of the process illustrated in Figure 1.

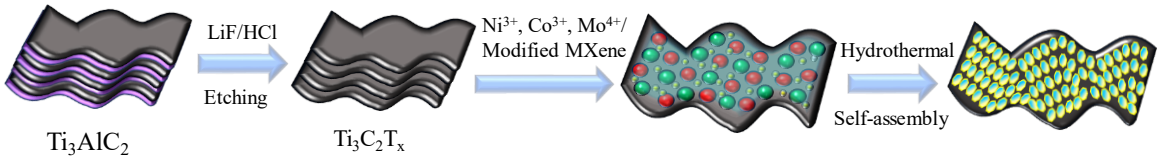

Figure 1. Schematic of the synthesis process of hierarchical NiCoMoPx/MXene nanostructure.

2.3 Physicochemical characterization

Scanning electron microscopy (Hitachi SU8010, Japan) and transmission electron microscopy (TEM, FEI Talos L120C) operating at 120 kV were used to examine the surface morphology and nanostructure, respectively. The elemental and particle distribution was observed through mapping analysis using SEM (TESCAN VEGA3, Czech Republic, with AZtec analysis software, Oxford Instruments, UK). X-ray photoelectron spectroscopy (XPS, Kratos AXIS Ultra) was employed to analyse the surface chemical states.

2.4 Electrocatalytic activities of the oxygen evolution reaction (OER)

OER performance was assessed in 1.0 M KOH using a typical three-electrode setup consisting of glassy carbon electrode (GCE) as working electrode, a graphite rod as the counter electrode, and Ag/AgCl (3 M KCl) as the reference electrode. Linear sweep voltammetry (LSV) was measured at 5 mV/s with 85% iR correction. Tafel plots were derived from LSV curves using the equation: $\eta = b \log(j) + \alpha$ (η: overpotential, j: current density, b: Tafel value, α: exchange current density). The electrochemically active surface area (ECSA) was determined from the electrochemical double-layer capacitance (C_{dl}) from a cyclic voltammetry test, calculated by plotting the current density differences ($\Delta j = j_a - j_c$) against various scan rates (5, 25, 50, 75, and 100 mV s^{-1}) in the non-faradaic region, where the slope corresponds to $C_{dl}/2$. ECSA was then estimated as ECSA = C_{dl}/C_s, assuming a specific capacitance (C_s) of 0.04 mF cm^{-2} for a flat electrode in alkaline electrolyte. The turnover frequency (TOF) was calculated by the equation: TOF = (J x A) / (4 x F x m), where J represents the current density (A cm^{-2}) at an overpotential of 350 mV, A and m represent the area of the electrode and the number of moles of the active materials. All potentials were calibrated using the reversible hydrogen electrode (vs RHE): $E_{RHE} = E_{Ag/AgCl} + 0.059\ pH + 0.197$. 5 mg of each sample was prepared for catalyst ink in a mixture of 150 µL DI water, 150 µL isopropanol, and 50 µL Nafion solution.

3. Results and discussion

3.1 Physicochemical characterization of layered double hydroxide Ni-based with MXene

The crystal structures of exfoliated $Ti_3C_2T_x$ flakes, NiCoMoP/MXene composites, and the parent MAX phase Ti_3AlC_2 were analyzed by X-ray diffraction (XRD) (Figure 2). The Ti_3AlC_2 MAX phase exhibits characteristic peaks at the (002), (004), (101), (104), (105), (107), (109), and (110) planes (JCPDS No. 52-0875). The absence of several higher-order peaks in the 2θ range of 30–50° and the reduction in intensity indicate the successful conversion of Ti_3AlC_2 into $Ti_3C_2T_x$ MXene via selective Al layer etching with HCl and LiF. The (002) peak of $Ti_3C_2T_x$ shifted from 9.5° to 6.5° is attributed to interlayer expansion induced by Al removal, surface termination groups, and Li^+ intercalation [11], with the shift reflecting increased interlayer spacing [12].

For the NiCoMoP/MXene composite, three distinct peaks at 44.52°, 51.96°, and 65.78° correspond to the (222), (200), and (211) planes of NiCo-LDH/NiCo phosphide (JCPDS No. 38-0715), confirming successful formation of NiCoMoP. The composite exhibits feature from both MXene and NiCo phases: the MXene (002) peak shifts slightly to lower angles, while NiCo-LDH/NiCoP peaks remain distinct, indicating strong interfacial coupling, Mo/P-induced lattice distortion, and intercalation of NiCoMoP nanoparticles between MXene layers. Compared to pristine NiCo-LDH, these modifications demonstrate partial integration of diffraction features, electronic redistribution, and surface reconstruction, which enhance electron transfer, structural stability, and catalytic activity during OER.

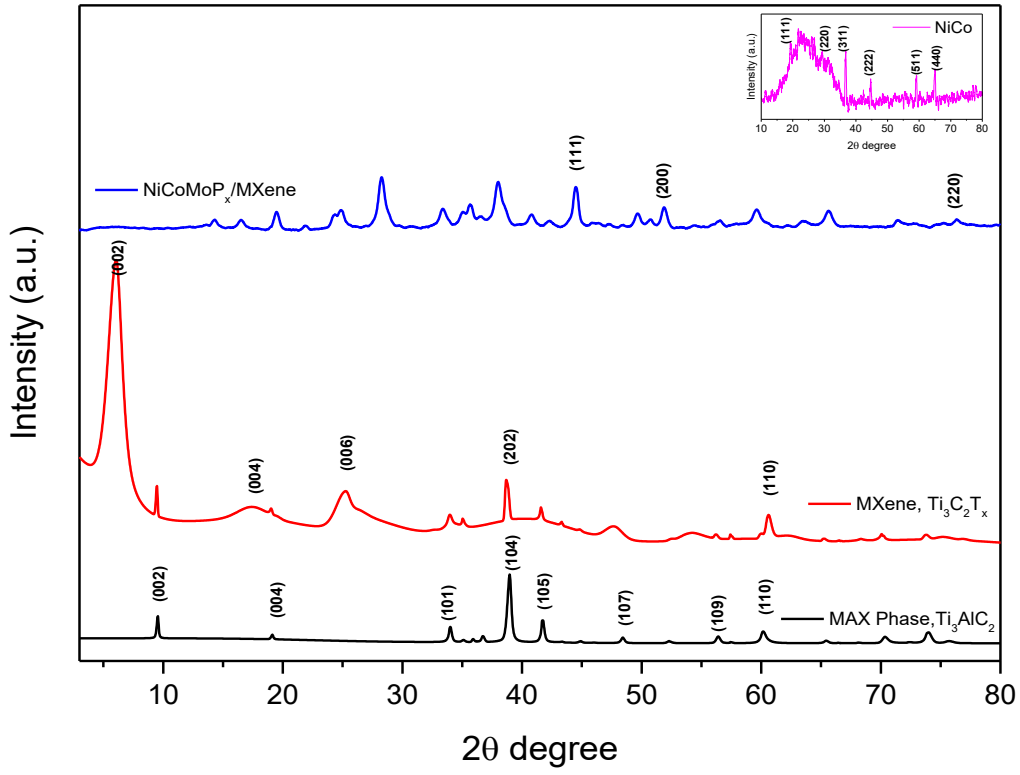

Figure 2. XRD patterns of the isolated $Ti_3C_2T_x$ flakes and $NiCoMoP_x$/MXene.

The morphology of the NiCoMoP/MXene and MXene was analysed using SEM and HRTEM, as depicted in Figure 3. Typically, the precursor Ti_3AlC_2 MAX phase was selectively etched by

using the HCl/LiF mixture to form isolated $Ti_3C_2T_x$ flakes, as shown in the SEM image in Figure 3a. The stacked layers of morphological features are clearly obtained when Al layers were successfully removed from the Ti_3AlC_2 MAX phase.

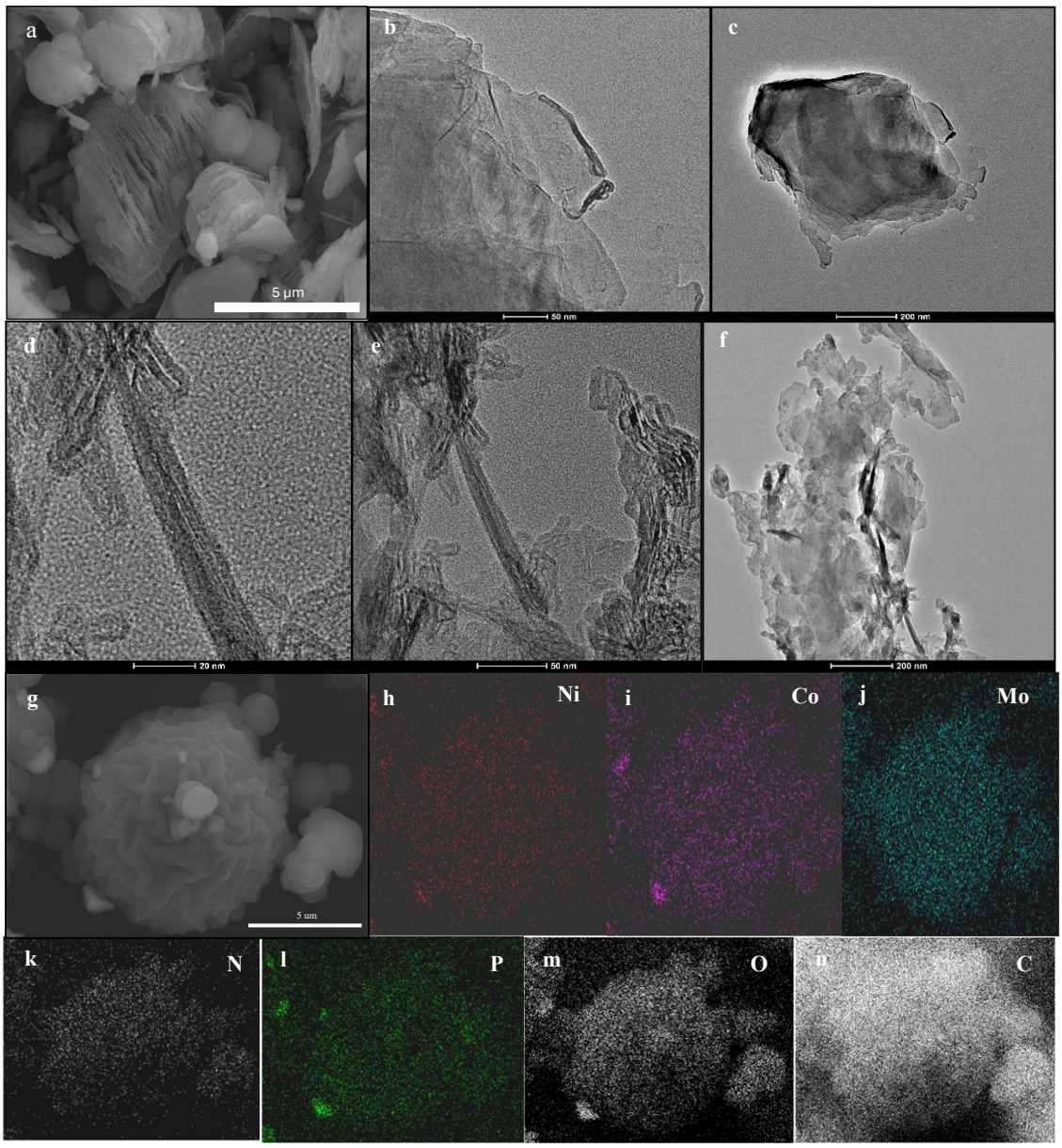

Figure 3. (a) SEM, (b) and (c) HRTEM images of a typical $Ti_3C_2T_x$ flakes structure, (d), (e), and (f) HRTEM image of NiCoMoP, and (g) SEM image of NiCoMoP with their mapping scan of elements (h), (i), (j), (k), (l), (m), and (n).

The high-resolution transmission electron microscopy (HRTEM), as shown in Figure 3b - c, further confirms the ultrathin nature of MXene nanoflakes. Following the in-situ growth of NiCoMoP on MXene, the structure is prone to aggregation and sized cluster production with having flower-like structure as portrayed in Figure 3h [9]. HRTEM images in Figure 3d–f were obtained to close up the morphology of NiCoMoP, which revealed a nanosheet-like structure that

was aggregated to form flower-like self-assembled structures, which is consistent with the SEM image. Furthermore, semi-quantitative mapping area analyses were conducted for a subset of areas, revealing the uniform distribution of Ni, Co, Mo, Ni, P, O, and C elements in NiCoMoP. This confirms the successful doping of the Mo element, and the heteroatom elements of P and N in developing a hybridize structure of NiCoMoP.

3.2 Electrocatalytic activities in oxygen evolution reaction (OER) of Ni-based with MXene

The OER activities of the prepared samples with manipulation of various molar ratios Ni-to-Co-to-Mo were denoted as $Ni_1Co_1Mo_{0.125}P$/MXene, $Ni_1Co_{0.75}Mo_{0.1}P$/MXene, $Ni_1Co_{0.5}Mo_{0.1}P$/MXene, and $Ni_1Co_{0.4}Mo_{0.1}P$/MXene and displayed in Figure 4. The $Ni_1Co_1Mo_{0.125}P$/MXene showed the highest current density produced with the lowest overpotential at η_{10} of about 314.6 mV, followed by 409.13 mV for $Ni_1Co_{0.4}Mo_{0.1}P$/MXene, and 419 mV for $Ni_1Co_{0.5}Mo_{0.1}P$/MXene. In contrast, the $Ni_1Co_{0.75}Mo_{0.1}$ P/MXene did not demonstrate satisfactory performance in OER.

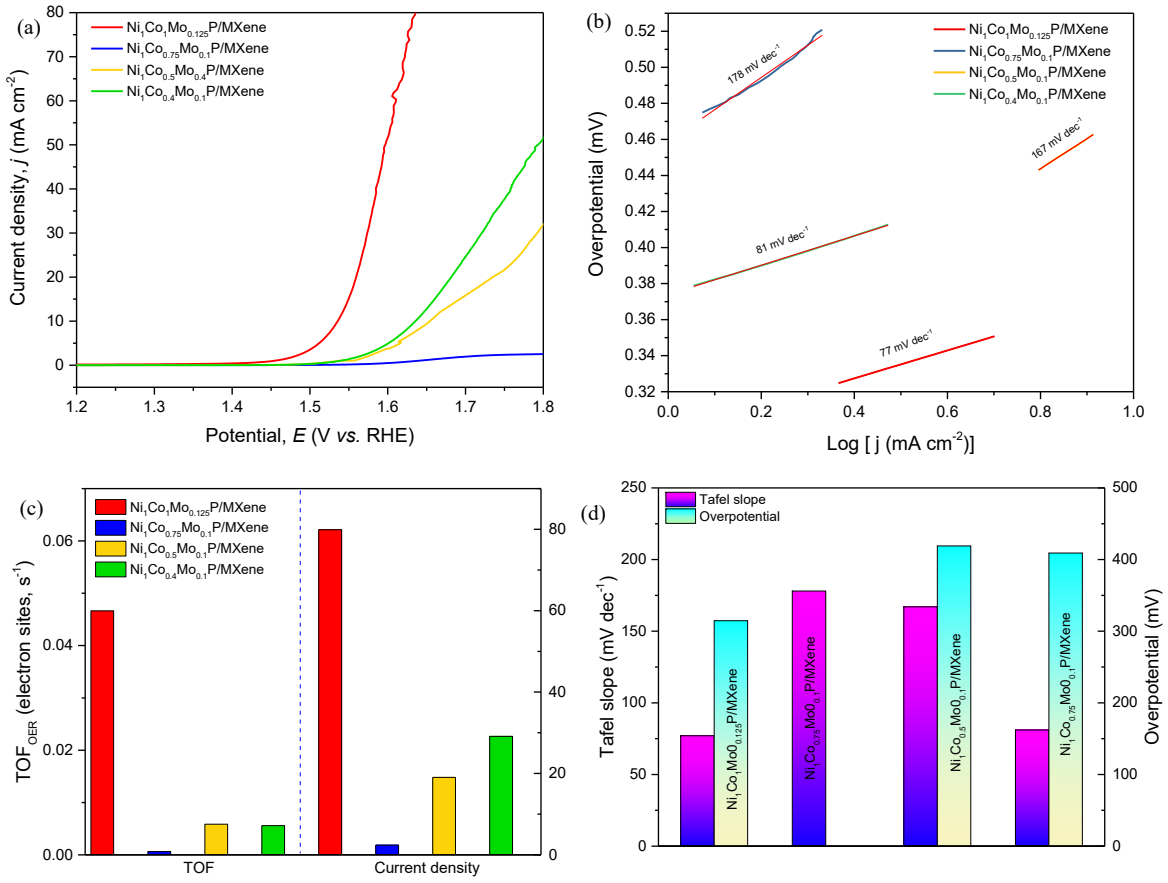

Figure 4. The electrocatalytic activities of OER in 1.0 mol/L KOH for electrocatalyst $Ni_1Co_1Mo_{0.125}P$/MXene, $Ni_1Co_{0.75}Mo_{0.1}P$/MXene, $Ni_1Co_{0.5}Mo_{0.1}P$/MXene, and $Ni_1Co_{0.4}Mo_{0.1}P$/MXene at scan rate 5 mV s^{-1} (a) LSV curve, (b) Tafel slope, (c) contrast histogram of TOF value and maximum current density, *j* (mA cm^{-2}) produced, (d) comparison of Tafel slope with η_{10}

Additionally, the OER kinetics was assessed by fitting the Tafel plots of the electrocatalysts using the Tafel equation, $\eta = \alpha + b \log j$. Here, η (V) represents the overpotential, α (V) is the intercept, b (mV dec^{-1}) is the Tafel slope, and *j* (mA cm^{-2}) is the current density. The $Ni_1Co_1Mo_{0.125}P$/MXene, $Ni_1Co_{0.75}Mo_{0.1}P$/MXene, $Ni_1Co_{0.5}Mo_{0.1}P$/MXene, and

$Ni_1Co_{0.4}Mo_{0.1}P$/MXene had Tafel slope values of 77, 178, 167, and 81 (mV dec-1), respectively. The $Ni_1Co_1Mo_{0.125}P$/MXene showed the fastest response rate with the lowest Tafel slope value, a low exchange current density, α (1.497 x 10-4 mA cm^{-2}), and a high turnover frequency (TOF) of 0.04664 s^{-1} at η = 400 mV. The higher TOF of $Ni_1Co_1Mo_{0.125}P$/MXene comes from the combined effects of its molecule components. The presence of Mo changes the electronic environment, lowering the adsorption energy barrier of OER intermediates. Meanwhile, Ni and Co provide many redox active sites. Phosphorus aids rapid charge transfer stabilizes the local coordination environment, and improves electron conductivity. These effects result in higher turnover frequencies compared to undoped versions. The combined contributions of the elements in $Ni_1Co_1Mo_{0.125}P$/MXene lead to its increased TOF. Ni and Co offer plentiful redox-active sites, while Mo helps tune the electronic environment, reducing the adsorption energy barrier of OER intermediates. Phosphorus boosts electron conductivity and stabilizes the local coordination environment, which supports rapid charge transfer. These factors yield higher turnover frequencies than undoped counterparts. This shows that the open structure around the active site NiCoMo allows for efficient mass transport and rapid charge transfer across these active sites during diffusion, including both inward and outward diffusion of oxygen and OH-. These findings highlight that the combination of Ni, Co, Mo, and P in the MXene is essential in determining its electrocatalytic activity for the oxygen evolution reaction.

The OER kinetics is further supported by the electrochemical double-layer capacitance C_{dl} analysis as measured in Figure 5a. The $Ni_1Co_1Mo_{0.125}P$/MXene exhibited the largest slope among the tested samples, with the C_{dl} value being the highest at 18.2 μF cm^{-2}, indicating it has a larger electrochemical surface area, which promotes OER activity, with an ECSA value is 0.728 cm^2. Electrochemical impedance spectroscopy (EIS) (in Figure 5b) further demonstrated that $Ni_1Co_1Mo_{0.125}P$/MXene possessed the smallest semicircle diameter, confirming its lowest charge-transfer resistance and superior interfacial electron transport kinetics [14]. The chronoamperometric stability test of the highest-performance $Ni_1Co_1Mo_{0.125}P$/MXene, as shown in Figure 5c, revealed only a slight current decay over extended operation, highlighting the excellent durability of the catalyst under continuous OER conditions. The kinetic parameters for all electrocatalysts in OER activities are presented in Table 1.

Table 1. Electrochemical parameters of prepared electrocatalysts NiCoMoP/MXene towards OER.

Electrocatalyst	η_{10} (mV)	Tafel slope (mV dec^{-1})	Exchange current density (mA cm^{-2}), α	Turnover frequency (TOF, s^{-1})	C_{dl} (μF cm^{-2})	ECSA (cm^{-2})
$Ni_1Co_1Mo_{0.125}P$/MXene	314.6	77	1.497 x 10^{-4}	0.04664	18.2	0.728
$Ni_1Co_{0.75}Mo_{0.1}P$/MXene	0	178	2.735 x 10^{-3}	6.317 x 10^{-4}	1.3	0.052
$Ni_1Co_{0.5}Mo_{0.1}P$/MXene	419.0	167	0.0140	5.8536 x 10^{-3}	5.2	0.208
$Ni_1Co_{0.4}Mo_{0.1}P$/MXene	409.13	81	2.504 x 10^{-5}	5.5763 x 10^{-3}	7.5	0.3

The benchmarking analysis in Figure 5d showed that the OER performance of NiCoMoP/MXene is similar to other electrocatalysts like CoS [15], CoP/N-CNT [16], $Ni_{2.5}Fe_{2.5}$-$P/Ti_3C_2T_x$ [17], $FeCoB_2$ [18], Co_3O_4/MXene [19], Ni-MOF@CNT [20], $Na_2Co_{0.75}Fe_{0.25}P_2O_7C$ NPs [21], and Ni-Fe-S/D-Ti_3C_2 [22]. This confirms that hierarchical Mo-doping and MXene coupling

effectively improve catalytic activity and stability. The initial study of the NiCoMoP/MXene electrocatalyst showed promising activity for the OER, suggesting it could be a strong candidate for further optimization. Additionally, testing different operating conditions might also enhance catalytic activity.

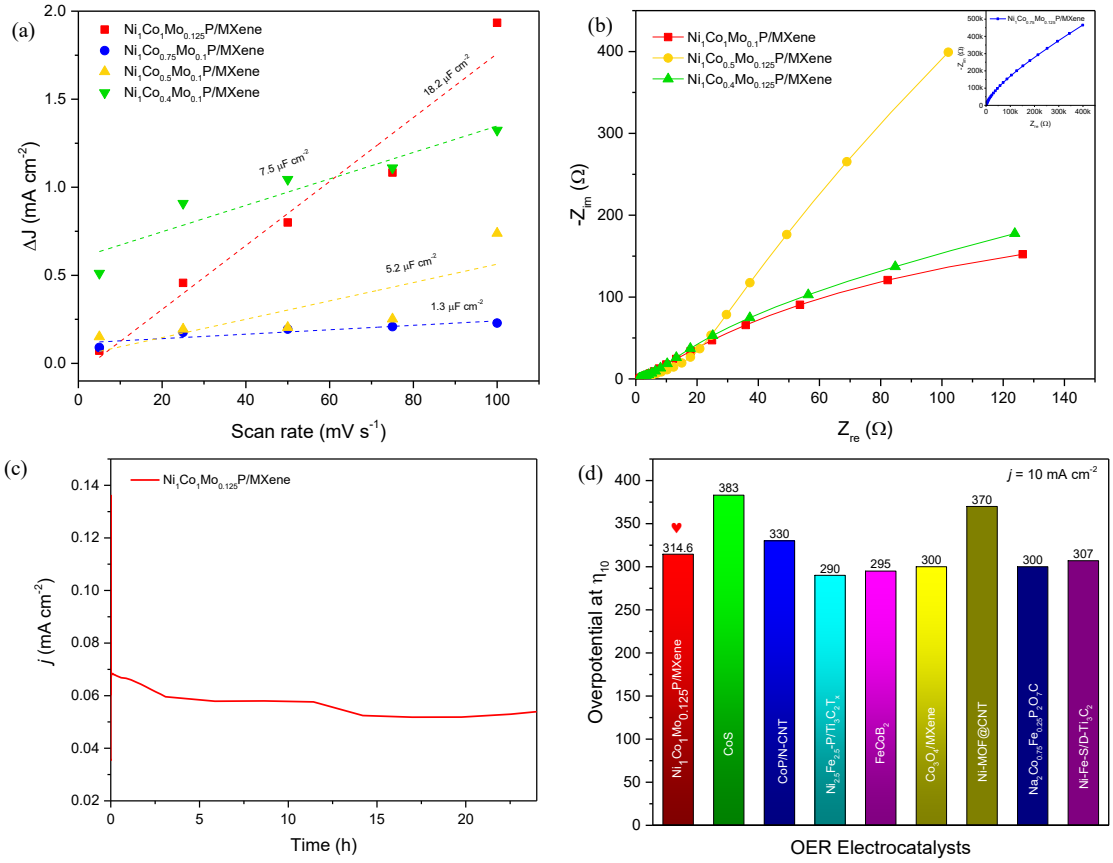

Figure 5. Electrochemical characterization of the NiCoMoP/MXene composite: (a) electrochemical double-layer capacitance (C_{dl}) from different scan rate, (b) electrochemical impedance spectroscopy (EIS), (c) chronoamperometry (CA) tests the stability of the electrocatalyst at a constant overpotential, and (d) comparison of the overpotential of the NiCoMoP/MXene with previously reported OER electrocatalyst performance.

Therefore, it is suggested to demonstrate the NiCoMoP/MXene functions in the OER mechanism reaction as illustrated in Figure 6. The oxygen evolution reaction (OER) over the $Ni_1Co_1Mo_{0.125}P$/MXene composite proceeds via a four-step mechanism. A highly conductive platform made possible by the multilayer MXene substrate speeds up electron transport to the active regions. Ni and Co atoms anchored on the MXene surface act as the primary catalytic centers, where hydroxide ions (OH^-) from the alkaline electrolyte are initially adsorbed. The nearby Mo atoms modulate the electronic structure of the Ni/Co sites, promoting charge redistribution and enhancing the adsorption strength of intermediates. Phosphorus incorporation further improves electronic conductivity and stabilizes the active sites. During the OER process, adsorbed OH^- species undergo stepwise deprotonation and O-O bond formation to generate the OOH^* intermediate. This intermediate then evolves into O_2 and is released into the

solution. MXene, Ni/Co, Mo, and P interact synergistically to enhance the kinetics of each elementary step, enhancing the overall catalytic activity and stability of the composite.

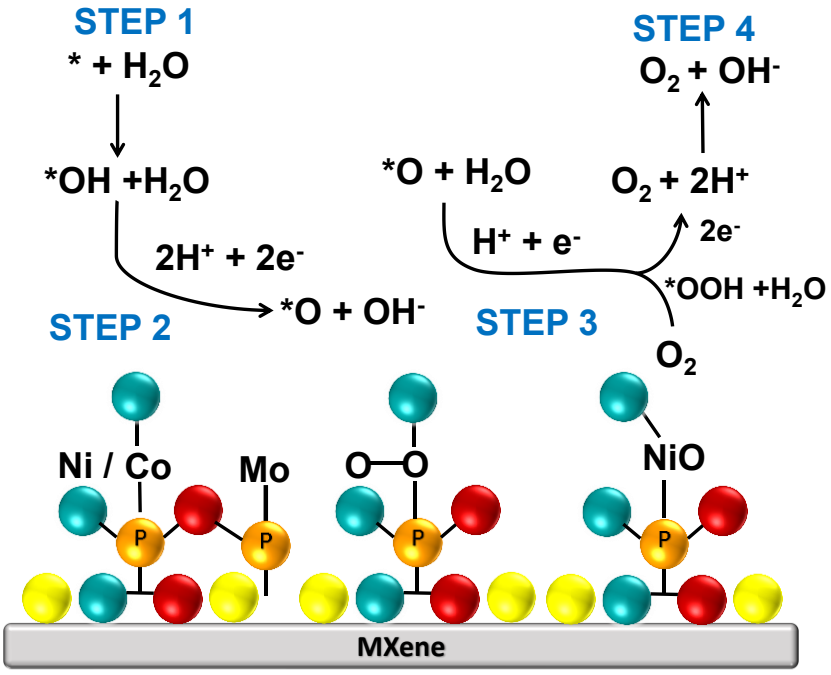

Figure 6. The schematic for NiCoMoP/MXene in the oxygen evolution reaction (OER) mechanism.

4. Conclusion

This study investigates the development of a hierarchical NiCoMoP/MXene nanohybrid electrocatalyst. It combines Mo-doped NiCo-based phosphides with the highly conductive and chemically active 2D $Ti_3C_2T_x$ MXene. The resulting flower-like nanostructures, averaging 200 to 300 nm, create plenty of electroactive sites and efficient electron transport pathways. Among the samples, the $Ni_1Co_1Mo_{0.125}P$/MXene showed good OER activity, achieving an overpotential of 314.6 mV to reach 10 mA cm^{-2} in the alkaline medium. It has a low Tafel slope of 77 mV dec^{-1}, a low exchange current density, α (1.497 x 10^{-4} mA cm^{-2}), and a high turnover frequency (TOF) of 0.04664 s^{-1} at η = 400 mV. These factors highlight its effective catalytic performance. The catalyst also has high double-layer capacitance (C_{dl}), which means it has a large electrochemically active surface area (ECSA) and a greater density of exposed active sites. Electrochemical impedance spectroscopy (EIS) showed that it has the lowest charge-transfer resistance among the tested samples, indicating fast charge transport and improved interfacial kinetics. Additionally, chronoamperometry (CA) demonstrated excellent stability with minimal performance decline, showing it maintains high structural integrity during extended OER operations. Overall, these results emphasize the advantages of incorporating Mo and using MXene support, creating a strong platform for developing non-noble electrocatalysts in water electrolysis and future energy conversion and storage technologies.

Acknowledgments

This work received support from the Fundamental Research Grant Scheme (FRGS) under grant number FRGS/1/2023/TK08/ UITM/02/12 and the Sunway University Internal Grant Scheme 2/2023 (GRTIN-IGS(02)-RCNMET-05-2023).

References

[1] Z. Chen, Y. Song, J. Cai, X. Zheng, D. Han, Y. Wu, Y. Zang, S. Niu, Y. Liu, J. Zhu, X. Liu, G. Wang, Tailoring the d-Band Centers Enables Co4N Nanosheets To Be Highly Active for Hydrogen Evolution Catalysis, Angew. Chemie - Int. Ed. 57 (2018) 5076–5080. https://doi.org/10.1002/anie.201801834.

[2] K. Liu, C. Zhang, Y. Sun, G. Zhang, X. Shen, F. Zou, H. Zhang, Z. Wu, E.C. Wegener, C.J. Taubert, J.T. Miller, Z. Peng, Y. Zhu, High-Performance Transition Metal Phosphide Alloy Catalyst for Oxygen Evolution Reaction, ACS Nano 12 (2018) 158–167. https://doi.org/10.1021/acsnano.7b04646.

[3] D. Xu, Z. Kang, H. Zhao, Y. Ji, W. Yao, D. Ye, J. Zhang, Coupling heterostructured CoP-NiCoP nanopin arrays with MXene (Ti3C2Tx) as an efficient bifunctional electrocatalyst for overall water splitting, J. Colloid Interface Sci. 639 (2023) 223–232. https://doi.org/10.1016/j.jcis.2023.02.052.

[4] X. Du, Y. Wang, Z. Ye, W. Wang, Y. Wang, Interface effect of MXene/CoP2 on oxygen evolution reaction, Mater. Lett. 360 (2024) 136024. https://doi.org/10.1016/j.matlet.2024.136024.

[5] J. Su, J. Zhou, L. Wang, C. Liu, Y. Chen, Synthesis and application of transition metal phosphides as electrocatalyst for water splitting, Sci. Bull. 62 (2017) 633–644. https://doi.org/10.1016/j.scib.2016.12.011.

[6] Q. Wang, N. Han, A. Bokhari, X. Li, Y. Cao, S. Asif, Z. Shen, W. Si, F. Wang, J.J. Klemeš, X. Zhao, Insights into MXenes-based electrocatalysts for oxygen reduction, Energy 255 (2022). https://doi.org/10.1016/j.energy.2022.124465.

[7] Y. Cheng, Y. Zhang, Y. Li, J. Dai, Y. Song, Hierarchical Ni2P/Cr2CT: X (MXene) composites with oxidized surface groups as efficient bifunctional electrocatalysts for overall water splitting, J. Mater. Chem. A 7 (2019) 9324–9334. https://doi.org/10.1039/c9ta00008a.

[8] J. Chen, Q. Long, K. Xiao, T. Ouyang, N. Li, S. Ye, Z.Q. Liu, Vertically-interlaced NiFeP/MXene electrocatalyst with tunable electronic structure for high-efficiency oxygen evolution reaction, Sci. Bull. 66 (2021) 1063–1072. https://doi.org/10.1016/j.scib.2021.02.033.

[9] B. Zhang, F. Yang, X. Liu, N. Wu, S. Che, Y. Li, Phosphorus doped nickel-molybdenum aerogel for efficient overall water splitting, Appl. Catal. B Environ. 298 (2021). https://doi.org/10.1016/j.apcatb.2021.120494.

[10] S. Song, Y. Wang, X. Liu, X. Tian, Y. Liu, X. Liu, F. Sun, Y. Yuan, W. Li, J. Zang, Synthesis of Mo-doped NiFe-phosphate hollow bird-nest architecture for efficient and stable seawater electrolysis, Appl. Surf. Sci. 604 (2022). https://doi.org/10.1016/j.apsusc.2022.154588.

[11] C. Huang, L. Yu, W. Zhang, Q. Xiao, J. Zhou, Y. Zhang, P. An, J. Zhang, Y. Yu, N-doped Ni-Mo based sulfides for high-efficiency and stable hydrogen evolution reaction, Appl. Catal. B Environ. 276 (2020). https://doi.org/10.1016/j.apcatb.2020.119137.

[12] N. Hao, Y. Wei, J. Wang, Z. Wang, Z. Zhu, S. Zhao, M. Han, X. Huang, In situ hybridization of an MXene/TiO2/NiFeCo-layered double hydroxide composite for electrochemical and photoelectrochemical oxygen evolution, RSC Adv. 8 (2018) 20576–20584. https://doi.org/10.1039/c8ra02349b.

[13] Y. Li, K. Dastafkan, Q. Sun, Y. Ma, X. Wang, X. Yang, Z. Wang, C. Zhao, Ni-based 3D hierarchical heterostructures achieved by selective electrodeposition as a bifunctional electrocatalyst for overall water splitting, Electrochim. Acta 379 (2021). https://doi.org/10.1016/j.electacta.2021.138042.

[14] G.B. Darband, M. Aliofkhazraei, A.S. Rouhaghdam, M.A. Kiani, Three-dimensional Ni-Co alloy hierarchical nanostructure as efficient non-noble-metal electrocatalyst for hydrogen evolution reaction, Appl. Surf. Sci. 465 (2019) 846–862. https://doi.org/10.1016/j.apsusc.2018.09.204.

[15] W. Adamson, C. Jia, Y. Li, C. Zhao, Cobalt oxide micro flowers derived from hydrothermal synthesised cobalt sulphide pre-catalyst for enhanced water oxidation, Electrochim. Acta 355 (2020). https://doi.org/10.1016/j.electacta.2020.136802.

[16] Z. Zewu, D. Yifan, C. Lijingxian, B. Jiakai, B. Xiaohai, B. Jiehua, CoP nanoparticles embedded in N-doped carbon for highly efficient oxygen evolution reaction electrocatalysis, Mater. Lett. 364 (2024). https://doi.org/10.1016/j.matlet.2024.136405.

[17] L. Tan, J. Wang, S. Zhou, H. Zhu, J. Guo, Y. Chen, X. Li, Z. Dong, Q. Zhang, Y. Cong, NiFe phosphides coupled on Ti3C2Tx MXene nanosheets for high-efficiency oxygen evolution reaction in alkaline medium, J. Colloid Interface Sci. 689 (2025) 137263. https://doi.org/10.1016/j.jcis.2025.137263.

[18] X. Zou, W. Zhang, X. Zhou, K. Song, X. Ge, W. Zheng, The surface of metal boride tinted by oxygen evolution reaction for enhanced water electrolysis, J. Energy Chem. 72 (2022) 509–515. https://doi.org/10.1016/j.jechem.2022.05.039.
[19] Y. Lu, D. Fan, Z. Chen, W. Xiao, C. Cao, X. Yang, Anchoring Co3O4 nanoparticles on MXene for efficient electrocatalytic oxygen evolution, Sci. Bull. 65 (2020) 460–466. https://doi.org/10.1016/j.scib.2019.12.020.
[20] T.V.M. Sreekanth, G.R. Dillip, P.C. Nagajyothi, K. Yoo, J. Kim, Integration of Marigold 3D flower-like Ni-MOF self-assembled on MWCNTs via microwave irradiation for high-performance electrocatalytic alcohol oxidation and oxygen evolution reactions, Appl. Catal. B Environ. 285 (2021) 119793. https://doi.org/10.1016/j.apcatb.2020.119793.
[21] H.J. Song, H. Yoon, B. Ju, D.Y. Lee, D.W. Kim, Electrocatalytic Selective Oxygen Evolution of Carbon-Coated Na2Co1-xFexP2O7 Nanoparticles for Alkaline Seawater Electrolysis, ACS Catal. 10 (2020) 702–709. https://doi.org/10.1021/acscatal.9b04231.
[22] K. Min, G. Lee, Y. Son, H. Seong, S.H. Baeck, Bimetallic nickel iron sulfide directly grown on defect-rich Ti3C2 MXene as an efficient bifunctional electrocatalyst for water electrolysis, Catal. Today 426 (2024) 114369. https://doi.org/10.1016/j.cattod.2023.114369.